Some properties of the elastic waves in quasiregular heterostructures

2002 J. Phys.: Condens. Matter 14 5933

(http://iopscience.iop.org/0953-8984/14/24/305)

INSTITUTE OF PHYSICS PUBLISHING JOURNAL OF PHYSICS: CONDENSED MATTER

J. Phys.: Condens. Matter **14** (2002) 5933–5957 PII: S0953-8984(02)34778-7

Some properties of the elastic waves in quasiregular heterostructures

V R Velasco[1,4], **R Pérez-Alvarez**[2] **and F García-Moliner**[3]

[1] Instituto de Ciencia de Materiales, CSIC, Cantoblanco, 28049 Madrid, Spain
[2] Departamento de Física Teórica, Facultad de Física, Universidad de La Habana, San Lázaro y L, Vedado 10400, Cuba
[3] Cátedra de Ciencia Contemporánea, Universidad Jaume I, 12071 Castellón de la Plana, Spain

E-mail: vrvr@icmm.csic.es

Received 12 March 2002
Published 31 May 2002
Online at stacks.iop.org/JPhysCM/14/5933

Abstract

The normal-mode spectrum of quasiregular structures has peculiar properties which have stimulated a great deal of research. The current situation is critically examined for the case of elastic waves. So far most of the research in this field appears to be theoretical. The roles of boundary conditions and of the constitutive material blocks are discussed, as well as the conditions required for reliable calculations of the topological properties of the spectra. The different quasiregular sequences more commonly studied may have significantly different formal properties, a fact not often considered. The relationship to other fields of physics is pointed out, the need for more experimental work is stressed, and, generally speaking, some directions for further research in the field are suggested.

1. Introduction

The traditional classification of solids into crystalline and amorphous underwent substantial revision due to the discovery of icosahedral alloys [1, 2] having symmetries forbidden for ordinary crystals. These systems, known as 'quasicrystals', are not periodically ordered like the ordinary crystals, but they are not disordered or amorphous systems. They exhibit a well defined discrete point group symmetry, like ordinary crystals, but incompatible with periodic translational order. The quasicrystals have a kind of translational periodicity known as quasiperiodicity. In fact they do not have long-range periodic translational order, but they do possess 'long-range positional order'. Some one-dimensional (1D) 'quasicrystals' have been found in Al–Cu–Co, Al–Ni–Si, and Al–Cu–Mn [3]. These systems have a 'periodic' in-plane structure, but the planes are stacked aperiodically following a Fibonacci sequence.

[4] Author to whom any correspondence should be addressed.

Different ways to obtain an aperiodic array of atoms in one dimension from a periodic square lattice in two dimensions can be found in [4]. This cut-and-projection method can be further generalized to crystalline approximants in two and three dimensions of quasicrystals. On the other hand, for almost 30 years research on quantum nanostructures has been very intensive [5,6]. As a result, epitaxial growth techniques have been developed and it is possible to obtain samples with prescribed design parameters and having high quality levels. These techniques have also been used to grow non-periodic digital heterostructures [7], and even quasiperiodic heterostructures [8–11]. The discovery of the quasicrystals and the realization of these quasiregular heterostructures stimulated in the early 1980s a good deal of theoretical study [12–22]. In these studies a linear one-dimensional chain of atoms was considered, and a study was made of the electronic states in a tight-binding model having one state per atom and having an on-site energy which can take one of two values E_A or E_B according to a prescribed sequence, while the hopping interaction is not changed. Some variations of this model were also considered. When the sequence follows a self-replicating rule the system is *quasiregular* or *quasiperiodic*, and the spectrum has novel and intriguing properties which resemble those of a simple Cantor set [23]. The most frequently studied case has been that of the Fibonacci sequence, for the reasons explained above, but other cases have also been studied and will be discussed here. The models could change—having for example the same atomic level but different hopping interactions—or one could study a different physical situation, like the longitudinal phonons in a one-dimensional chain having atomic masses m_A and m_B following the prescribed sequence. Basically all the systems considered in the former works amounted to academic problems, but the peculiar features and trends exhibited by the energy spectra pointed to the existence of some interesting basic features in the properties of non-periodic but quasiregular systems. This generated new research considering 'real' systems described in terms of simple models [24–27], and was also aided by the actual production of quasiregular heterostructures [8–11]. The work on different aspects of the spectra of quasiregular heterostructures has continued to be very active and many references can be found in [28,29]. These works have considered further aspects of the academic problems, but in many cases they have centred on actual physical systems, with varying degrees of elaboration in the models employed [30–54]. As compared with the abundant theoretical work, the experimental work associated with quasiregular systems remains scarce [33, 55–57].

On the other hand, many interesting mathematical studies of the physical properties of quasiregular systems have been published in the last few years [58–65]. In order to illustrate the main features of the quasiregular systems we shall concentrate on the elastic wave problem. In this way, it will be possible to study the physical properties of the quasiregular systems in a somewhat more realistic way than with strictly one-dimensional chains.

In section 2 we shall introduce some of the more common sequences which generate quasiregular systems. In section 3 we shall briefly discuss the different mathematical methods and theoretical approaches employed in the study of quasiregular systems. In section 4 we shall discuss the properties of elastic waves in quasiregular systems. Final comments and open questions will be presented in section 5.

2. Quasiregular sequences and systems

The historically first quasiregular sequence was introduced by Lorenzo Fibonacci in the thirteenth century. This produced the *Fibonacci numbers* according to the sequence

$$F_n = F_{n-1} + F_{n-2}. \tag{1}$$

Table 1. Substitution rules, and some low-order generations, for the most frequently studied quasiregular sequences. The first term is always assumed to be A.

Sequence	$\xi(A)$	$\xi(B)$	$\xi(C)$	$\xi(D)$	Generation
Fibonacci	AB	A			$S_6 = ABAABABAABAAB$
Thue–Morse	AB	BA			$S_4 = ABBABAABBAABABBA$
Period doubling	AB	AA			$S_4 = ABAAABABABAAABAA$
Circular	CAC	$ACCAC$	$ABCAC$		$S_2 = ABCACCACABCAC$
Rudin–Shapiro	AC	DC	AB	DB	$S_4 = ACABACDCACABDBAB$

Given the first two numbers, equation (1) determines the value of the generic number F_n for the nth generation in the sequence. It can be shown that

$$\lim_{n\to\infty} \frac{F_n}{F_{n-1}} = \frac{1+\sqrt{5}}{2} = \tau \tag{2}$$

where τ is the *golden ratio*.

It is easy to see how a heterostructure can be generated from the Fibonacci sequence. Let A be a slab of a given material, or materials, and B a slab of a different material, or materials. By expressing equation (1) as the juxtaposition of F_{n-1} and F_{n-2} we obtain

$$F_n = F_{n-1} \oplus F_{n-2}, \tag{3}$$

giving the resulting structure for generation n formed with A- and B-slabs, and having as starting seeds $F_0 = A$ and $F_1 = B$, for example. In this way it is possible to build a *quasiregular heterostructure* following a prescribed *quasiregular sequence*. This heterostructure is not a regular periodic one, but the prescription for higher generations contains a self-replicating law. Both A and B can be simple or composite, i.e. consisting of more than one slab of different materials [8–11].

The mathematical structure of the *quasiregular sequence* determines some basic properties and some theorems [59,65], which provide a formal basis on which to study the key features of the spectra of the *quasiregular heterostructures*. In order to describe quasiregular sequences it is quite common to introduce an alphabet [65] $\mathcal{A}$ formed by a number of *letters* allowing one to form words, and from them the infinite quasiregular heterostructure is formed. It is then only needed to define the first term and a *substitution rule* mapping the alphabet $\mathcal{A}$ onto a set of words of finite length [65]. In the case of the Fibonacci sequence [64, 66] the alphabet $\mathcal{A}$ consists of two letters A and B, and the substitution rule is given by

$$\xi(A) = AB, \qquad \xi(B) = A, \tag{4}$$

mapping $\mathcal{A}$ onto the set of words of finite length $\{AB, A\}$. It then suffices to define the first term $S_1 = A$ and successive applications of equation (4) yield the successive generations. This can be defined even more generally; for example AB in equation (4) can be replaced by AB^m, m being an integer >1, although $m = 1$ is the more usual case in physics.

Many other *quasiregular sequences* can be found in this way, with different alphabets and substitution rules. The most frequently studied cases are the Thue–Morse [21, 64, 66, 67], Rudin–Shapiro [21, 64–66, 68], period-doubling [21, 62, 64], circular [21, 64–66], binary non-Pisot [64, 66, 69], and ternary non-Pisot [64, 66, 69] ones. Table 1 summarizes for the most common of these sequences the substitution rules and gives typical examples of a low-order S_n for each one. By convention we have taken $S_1 = A$ and we have applied successively the rule $S_n = \xi(S_{n-1})$ following the prescriptions given in the table for each case. In this way it is possible to see the different degrees of complexity in the quasiregular heterostructures.

3. Mathematical methods and techniques

In order to study the spectra of quasiregular sequences several mathematical methods have been employed. Among them the *transfer matrix* methods have played a very important role. These methods are given many different names in the literature. If one writes down the form of the eigenfunction as a linear combination of given basic functions, often plane waves, half of them propagating, or decaying, in one direction and the other half in the opposite direction, then the transfer matrix is defined [70,71]; it transfers the coefficients of this combination from one point to another. Another different concept of the transfer matrix is as that matrix which transfers the function itself and its derivative with respect to some coordinate from one point to another. A preliminary account of this transfer matrix was given in [72] for the case of constant potential. The mathematical properties of this transfer matrix were studied in detail in [73] with emphasis on the Schrödinger equation, although the formal theory is equally valid for any linear second-order differential equation and for a set of coupled linear first-order differential equations. Transfer matrices have been very useful in the study of various exactly solvable models in statistical and quantum mechanics [74–76]. It is then quite natural to use transfer matrices to study the spectra of quasiregular heterostructures. Thus if ψ and ψ' are known at some initial point z_0, then for any z,

$$\begin{bmatrix} \psi(z) \\ \psi'(z) \end{bmatrix} = \mathbf{M}(z, z_0) \begin{bmatrix} \psi(z_0) \\ \psi'(z_0) \end{bmatrix}. \tag{5}$$

This defines $\mathbf{M}$ as the transfer matrix. For discrete systems described in terms of finite-difference equations, like a vibrating linear chain, the relationship defining $\mathbf{M}$ involves the amplitude at two different consecutive points. Thus

$$\begin{bmatrix} \psi(n) \\ \psi(n-1) \end{bmatrix} = \mathbf{M}(n, n_0) \begin{bmatrix} \psi(n_0) \\ \psi(n_0-1) \end{bmatrix}. \tag{6}$$

It must be stressed that all the fundamental mathematical studies of the properties of quasiregular systems apply to cases with a 2×2 *unimodular* transfer matrix. Thus it is clear that as regards the physics this approach is restricted to a class of problems in which there is only one amplitude or component. In this category fall problems such as: electrons states in the one-band tight-binding model; and purely longitudinal or purely transverse phonons of linear atomic chains following a quasiregular sequence. For continuous systems described by differential equations, similar problems would be: the one-band effective-mass Schrödinger equation; the Poisson equation for a simple dielectric model (plasmons in a phenomenological model of the electron gas or polar optical modes in a simple model for ionic crystals); pure transverse acoustic modes; etc. Another way to study the mathematical properties of the spectra of quasiregular systems has been through the so-called *trace map* [60,62,64,65,77–89].

To arrive at this concept we must note that the problem under study has two ingredients:

(i) the nature of the quasiregular sequence, as defined in the initial alphabet and the substitution rules; and
(ii) the *simple* nature of the problem defined on the given quasiregular sequence, which means that we are dealing with unimodular 2×2 transfer matrices.

In this case the application of the *Cayley–Hamilton* theorem

$$\mathbf{M}^2 - (\operatorname{tr}\mathbf{M})\mathbf{M} + \mathbf{I} = 0 \tag{7}$$

yields the following relations [90]:

$$\operatorname{tr}(\mathbf{M}_1\mathbf{M}_2) = \operatorname{tr}(\mathbf{M}_1)\operatorname{tr}(\mathbf{M}_2) - \operatorname{tr}(\mathbf{M}_1^{-1}\mathbf{M}_2), \tag{8}$$

$$\operatorname{tr}(\mathbf{M}^2) = (\operatorname{tr}(\mathbf{M}))^2 - 2, \tag{9}$$

$$\operatorname{tr}(\mathbf{M}_1\mathbf{M}_2\mathbf{M}_1\mathbf{M}_3) = \operatorname{tr}(\mathbf{M}_1\mathbf{M}_2)\operatorname{tr}(\mathbf{M}_1\mathbf{M}_3) - \operatorname{tr}(\mathbf{M}_2)\operatorname{tr}(\mathbf{M}_3) + \operatorname{tr}(\mathbf{M}_2\mathbf{M}_3), \tag{10}$$

$$\operatorname{tr}(\mathbf{M}_1^2\mathbf{M}_2) = \operatorname{tr}(\mathbf{M}_1)\operatorname{tr}(\mathbf{M}_1\mathbf{M}_2) - \operatorname{tr}(\mathbf{M}_2), \tag{11}$$

$$\mathbf{M}^3 = (\operatorname{tr}(\mathbf{M}))^2\mathbf{M} - \mathbf{M} - \operatorname{tr}(\mathbf{M})\mathbf{I}, \tag{12}$$

$$\operatorname{tr}(\mathbf{M}^3) = (\operatorname{tr}(\mathbf{M}))^3 - 3\operatorname{tr}(\mathbf{M}). \tag{13}$$

From these relations we can build now the *trace map*. Denote the nth generation S_n of a given quasiregular sequence by A_n/B_n, when the starting generation is $S_1 = A/B$ and associate a transfer matrix denoted by $\mathcal{A}_n/\mathcal{B}_n$ with the nth generation in each case. Then the substitution rules for the sequence induce recurrence relations between the transfer matrices for the successive generations. For instance, in the Fibonacci sequence, from equation (4) we obtain

$$\mathcal{A}_n = \mathcal{B}_{n-1}\mathcal{A}_{n-1}, \tag{14}$$

$$\mathcal{B}_n = \mathcal{A}_{n-1}. \tag{15}$$

These recurrence relations can be very useful in practice in doing actual calculations, but they also prove useful for allowing one to deduce a similar relation between their traces. We define in all cases

$$x_n = \operatorname{tr}(\mathcal{A}_n), \qquad y_n = \operatorname{tr}(\mathcal{B}_n). \tag{16}$$

The application of the substitution rules makes it necessary, in general, to introduce new traces. In the Fibonacci case it is necessary to introduce another trace:

$$z_n = \operatorname{tr}(\mathcal{A}_n\mathcal{B}_n) \tag{17}$$

and since from (14)–(15)

$$x_{n+1} = z_n \tag{18}$$

$$y_{n+1} = x_n \tag{19}$$

another recurrence relation for z_n is needed. In general this process brings into the analysis further traces, but the relations (7)–(13) can be used to break the chain. In [66] it was proved that for simple problems it is always possible to limit the chain to a finite number of matrices and traces. In the Fibonacci case, from (17) and (11) and making use of the cyclic invariance of the trace, it is readily obtained that

$$z_{n+1} = x_n z_n - y_n. \tag{20}$$

Equations (18)–(20) constitute a limited trace map for the Fibonacci sequence and involve a finite number of traces corresponding to a finite number of matrices (three in the present case), namely $\mathcal{A}_n$, $\mathcal{B}_n$, and $\mathcal{A}_n\mathcal{B}_n$. The corresponding finite set of words $\{A, B, AB\}$ is said to constitute the *lexicon* of the sequence [64]. The form of the trace map is not unique and can be cast in different ways. The important fact is that simple problems always have an associated trace map [66]. It is customary to cast the trace map in a more concise form which we shall call the *compact trace map*.

In the Fibonacci case, by eliminating y- and z-terms, equations (18)–(20) can be condensed into a recurrence formula for x_n, given by

$$x_n = x_{n-1}x_{n-2} - x_{n-3}, \tag{21}$$

which is the compact trace map for the Fibonacci sequence.

This case serves to illustrate the concept, although more general and complicated situations can be found. A detailed analysis is given in [29].

Decimation techniques based on the renormalization group have also been used [19, 28, 31].

For many interface systems, the Green function techniques have been very useful [91–93]. Quite recently a technique blending the surface Green function matching and the transfer matrix methods has been put forward [94] and employed to study 'real' quasiregular systems [50, 52–54]. The formal aspects of the method are presented in [52, 94] and will not be repeated here.

It is convenient now to consider a basic property of the eigenvalue spectrum of a problem, assumed to be simple in the sense explained before. Consider, for instance, the electronic state eigenvalues of a periodic superlattice. The spectrum consists of minibands and is piecewise continuous. In fact it is *absolutely continuous*, this meaning that given any point of the spectrum and any small interval about this point, all the points of the interval belong to the spectrum. The obvious exceptions are the miniband edges, for which the intervals must be one sided, just as in the case of the free-electron spectrum for the lower bound of the one band of states. The result is that on the real line the points of the spectrum form a one-dimensional set. Let us consider now a different situation: given any point of a spectrum, in any arbitrarily small interval about it there are always points of the spectrum, but not all points of the interval belong to it. Then the spectrum is *singular continuous*, this meaning that its points no longer cover the intervals of the real line densely as in the absolutely continuous case. These qualitative features can be complemented with some more precise characteristics. In the case of the *absolutely continuous* spectrum, a sampling of the set gives that in the neighbourhood of all the points the number of points is always proportional to the interval width. On the other hand, in the *singular continuous* spectrum, the number of points is proportional to a given power of the interval width. This power coefficient is the scaling index characterizing the point in the set. This fundamental property makes the spectra of some quasiregular systems different from that of a regular superlattice. In this way, given a quasiregular sequence, the *Bovier–Ghez theorem* [65] establishes that if some conditions are satisfied, then the spectrum of any simple problem defined on it is singular continuous. In this analysis the structure of the trace map plays a central role. By studying this it can be found that the periodic and Rudin–Shapiro sequences given in table 1 do not satisfy the conditions of the theorem. Thus one cannot prove whether the spectrum is or is not singular continuous. In fact, for the superlattice it is known to be absolutely continuous.

All the problems considered here are described by linear equations, but the mathematical analysis is based on the study of the trace maps, which consist of *non-linear* equations. Thus there are some affinities with the study of chaotic phenomena described in terms of non-linear dynamics. This similarity is particularly clear with respect to the topological properties of singular continuous spectra. In an abstract way the term *event* may mean either finding an eigenvalue in an interval of the real line or having a dynamical trajectory pass through an elementary domain in a phase space. In the nomenclature employed by some authors [12] the trace map is defined as the dynamical system under study. The fact, mentioned above, that singular continuous spectra do not cover the intervals of the real axis densely means that such spectra are fractal, with a dimension less than unity. Abundant examples of fractal analysis can be found in the literature on non-linear dynamics [95–98]. We shall present here a brief resume of some basic definitions and relations employed in the study of quasiregular systems.

Let $\{\omega_i\}$ $(i = 1, 2, \ldots, N)$ be a set of points on the real axis which we shall call the *spectrum*, although it could be any geometrically defined set of points. Consider the interval, or set of intervals, occupied by the spectrum, define elementary intervals (one-dimensional boxes) of size Ω, and cover the entire interval, or set of intervals, with $\mathcal{N}(\Omega)$ boxes of size Ω. Let q be a continuous parameter ranging from $-\infty$ to $+\infty$ and p_j be the fraction of points in box j.

The *generalized information of order q* is defined as [98]

$$I(\Omega, q) = \frac{1}{1-q} \log \sum_{j=1}^{\mathcal{N}(\Omega)} p_j^q, \tag{22}$$

and from this the *generalized box-counting dimension*

$$D_q = -\lim_{\Omega \to 0} \frac{I(\Omega, q)}{\log(\Omega)}. \tag{23}$$

Different concepts of dimension are defined in the literature, but for the purposes of this work it suffices to consider this and the *simple box-counting dimension* D_{bc} defined as follows. We consider the spectrum again, and cover it with $\mathcal{M}(\Omega)$ boxes of size Ω. Then [97, 98]

$$D_{bc} = -\lim_{\Omega \to 0} \frac{\log[\mathcal{M}(\Omega)]}{\log[\Omega]}. \tag{24}$$

The difference between $\mathcal{N}(\Omega)$ and $\mathcal{M}(\Omega)$ is that the latter, by definition, does not include any empty box, i.e. with no point of the spectrum in it. It can be shown [97, 98] that

$$D_{q=0} \equiv D_0 = D_{bc} \tag{25}$$

and this, under rather general conditions, is also equal to the *simple Hausdorff dimension* [95–98].

In the simplest, ideal case, D_q does not depend on q and we have just one fractal dimension D_0.

A property usually claimed for the spectra of quasiregular systems is that of *self-similarity*. It is important to stress the link of this property with the fractal analysis [95]. In a simple fractal object, if one looks at some fraction of it at some level of magnification, it is identical to any other fraction at some other level of magnification. Thus, after magnification it is impossible to tell which length scale one is seeing because there are no differences. It is proved [97] that self-similar sets have a fractal dimension D_q independent of q. This situation is rather exceptional and the more general situation must be described in terms of a *multifractal* analysis [95–97].

In order to do this, let p_j be the fraction of points of a given set which are contained in the jth cell of size Ω_j. It is assumed that $p_j(\Omega_j)$ satisfies a scaling relation of the form

$$p_j(\Omega_j) = k\Omega_j^{\alpha_j}, \tag{26}$$

where k is a proportionality constant and α_j is the *scaling index* for cell j. The different cells are now labelled to indicate that one is focusing on different regions of the spectrum, but the problem is analysed in the limit in which all $\Omega_j \to \Omega \to 0$. Then the number of cells $\mathcal{N}(\Omega)$ increases and the distribution of values of the α_j becomes continuous, so $n(\alpha)\,\mathrm{d}\alpha$ is the number of cells having a scaling index between α and $\alpha + \mathrm{d}\alpha$.

At this stage the crucial assumption is made that $n(\alpha)$ scales with the size of the cells according to a power law of the form

$$n(\alpha) = K\mathrm{e}^{-f(\alpha)}. \tag{27}$$

The proportionality constant K is irrelevant and $f(\alpha)$ can be interpreted as the fractal dimension of the partial set of points with scaling index α. The characteristic exponent $f(\alpha)$ [14] is of central importance in the multifractal analysis and is related to D_q. The basic properties of a multifractal object are

(i) D_q varies with q;
(ii) the scaling index α takes different values and, correspondingly, so does $f(\alpha)$; and

(iii) the object is no longer self-similar although some particular choice in the way of effecting a magnification might give an impression of self-similarity which does not hold up when more careful tests are performed [96].

The following relations can be proved [95–98] among D_q, α, and $f(\alpha)$:

$$f(\alpha) = q\frac{\mathrm{d}}{\mathrm{d}q}[(q-1)D_q] - (q-1)D(q) \tag{28}$$

$$\alpha(q) = \frac{\mathrm{d}}{\mathrm{d}q}[(q-1)D_q] \tag{29}$$

$$D(q) = \frac{1}{q-1}[q\alpha(q) - f(\alpha(q))]. \tag{30}$$

It can also be proved in a very general way that

$$D_{\max} = D(-\infty) \leqslant 1 \qquad D_{\min} = D(+\infty) \geqslant 0. \tag{31}$$

Moreover, α spans a range of values with lower and upper bounds [97]

$$\alpha_{\min} = D_{\min} \qquad \alpha_{\max} = D_{\max} \tag{32}$$

where $f(\alpha) > 0$.

The analysis starts from a given spectrum, resulting from an experiment or calculation, and one directly evaluates D_q numerically, and then, in principle, from (27)–(29) it could be possible to evaluate $f(\alpha)$. Practical aspects of the numerical calculation of $D(q)$ and $f(\alpha)$ were discussed in [29].

It should be stressed that the theory of all the mathematical and formal properties of quasiregular systems holds for infinitely large sequences, and this never actually happens in experiments or calculations. In practice we always deal with a 'high' but finite realization. A finite realization is the nth generation which results from applying the substitution rule n times and this is what one grows experimentally and what one calculates. If n is sufficiently large, one can assume that the description of the properties of the quasiregular systems will be reasonably accurate.

The set-up of the calculations raises the question of the boundary conditions. It is possible to take a finite generation S_n of the quasiregular system under study, to impose periodic boundary conditions, and to perform the analysis for a superlattice having S_n as the period. In other cases we can consider the finite S_n-system with different boundary conditions at the limiting interfaces. The alphabet letters entering in the sequence controlling the quasiregular systems grown experimentally can be composed of just one material [10] or of two different materials [8, 9, 11]. All these factors can have an influence on the analysis of the physical properties of quasiregular systems.

4. Elastic waves in quasiregular systems

Elastic waves constitute a very good testing ground for studying the properties of the spectrum of 'real' quasiregular heterostructures. In the range of validity of the elastic theory we shall have a rigorous description of the systems considered and we shall be able to study the influences of the different boundary conditions, constituent materials, etc, quoted at the end of the previous section.

In studying the basic properties of quasiregular systems it is possible to consider the materials isotropic or having high symmetry (cubic or hexagonal) and then study a high-symmetry direction. This will simplify the calculations without diminishing the physical insight of the study. In this way it is possible to consider quasiregular systems grown

along a given spatial direction, but having a perfect periodicity in the planes perpendicular to the growth direction. If the waves propagate along the x-direction, the transverse elastic displacement along the y-direction is uncoupled from the elastic displacements along the x- and z-directions. In this way the study of the elastic waves gives us a close parallel to the one-dimensional versions of the 'simple' models discussed before, the transverse u_y-displacement being described by a linear second-order differential equation. Associated with the same physical problem we have a more complicated situation linked to the sagittal waves having (u_x, u_z) coupled displacements, and described by two coupled linear second-order differential equations. In all cases, there are *matching boundary conditions* to be imposed at the coupling interfaces, expressing the continuity of the vibrational amplitudes and the normal components of the stress tensor. Note that these may, and often are, different from the *end boundary conditions*, here simply called boundary conditions, at the extremes of the finite realization of the heterostructure.

Some studies on the Raman spectra and transmission coefficients of the elastic waves in Fibonacci superlattices have been made in the last few years [27, 99–101]. In [46] the sagittal elastic waves in Fibonacci superlattices having periods up to that of the seventh generation were studied. It was found there that the structure of the frequency spectrum, as seen in the one-dimensional calculations, and presenting a succession of principal gaps and a 'self-similar' structure reflected in the presence of the secondary gaps, was not seen in the dispersion relations considered there. That was mainly due to the mixing of the two polarizations, one longitudinal and one transverse, entering the sagittal waves and to the low order of the generations included in [46]. It is interesting to note here something about the representation of the spectra. In the case of a regular superlattice the customary representation for the spectrum of the elastic waves is as a dispersion relation—that is to say, the frequency eigenvalues versus the wavevector in the growth direction, or in any other given direction. On the other hand, in the studies of one-dimensional models of quasiregular heterostructures it is quite common to represent the frequency eigenvalues versus a label which takes successive integral values and serves to identify the eigenvalues. Although quite often this is referred to as a dispersion relation, that must be understood as explained above.

In order to see the spectrum of the elastic waves in quasiregular heterostructures in 'real' systems but including higher generations, in [47] hexagonal crystals of the 6mm class were chosen. The study was centred on the transverse elastic waves of Fibonacci superlattices formed by hexagonal crystals of the 6mm class with the geometry associated with the existence of Bleustein–Gulyaev waves [102–104] in order to see the possible effects of the piezoelectricity on the transverse elastic wave spectrum. In that case the c-axis is parallel to the z-direction while y is the direction normal to the interface, and x is the propagation direction. In this case there is a decoupling between the motion along the x- and y-directions, corresponding to the sagittal waves studied in [46] and the motion along the z-direction due to the symmetry [104]. The transverse waves associated with the elastic displacement u_z were then studied in [47]. The Fibonacci superlattices studied there were obtained by stacking recursively along the y-direction with two generators, blocks A and B, mapping the mathematical rule in the Fibonacci sequence as given in table 1.

The materials considered were CdS and ZnO. The blocks A and B were formed by $(\mathrm{CdS})_i/(\mathrm{ZnO})_j$ layers and $(\mathrm{CdS})_i/(\mathrm{ZnO})_k$ layers respectively. The thicknesses of the different layers were $d(\mathrm{CdS}) = 17$ Å and $d(\mathrm{ZnO}) = 42$ Å for block A and $d(\mathrm{CdS}) = 17$ Å and $d(\mathrm{ZnO}) = 20$ Å for block B. In this way structures similar to the experimentally grown Fibonacci superlattices [8] were considered. Different realizations of the Fibonacci superlattices with increasing generation number, up to the thirteenth generation including 754 material slabs, were studied. Because of the finite size of the quasiregular systems considered,

in spite of the high number of material slabs included, two types of system with different boundary conditions were studied:

(a) infinite periodic superlattices having as period a given Fibonacci sequence; and
(b) a finite structure formed by a given Fibonacci sequence, with stress-free bounding surfaces.

The results thus obtained can be illustrated in a graphic way. Figure 1 gives a range of frequency values versus its ordering number for increasing frequencies, for periodic superlattices having as period the seventh (42 slabs), tenth (178 slabs), and thirteenth (754 slabs) generations of the Fibonacci sequence, respectively, corresponding to the superlattice Γ point. The figure displays the customary series of primary and secondary gaps for all the generations included in the study. Thus, some kind of 'self-similar' structure is then present in the frequency spectrum. The same structure was obtained for the $qD = \pi/2$ and $qD = \pi$ points, D being the superlattice period.

In figure 2 the same information as presented in figure 1 is given but for the finite Fibonacci generations, with the same number of slabs as in figure 1, having stress-free bounding surfaces. The same structure of the frequency spectrum is seen in figure 2 although the eigenvalues exhibit differences from those of the periodic case, induced by the different boundary conditions. The isolated points seen in the primary gaps, and also present in the secondary gaps, correspond to localized states. This can be seen in figure 3 representing the local density of states (LDOS) in arbitrary units of the $\omega = 14.37$ GHz mode of the finite tenth-generation Fibonacci superlattice versus the length of the multilayer system, having 55 A-blocks and 34 B-blocks, thus totalling a length of 4503 Å. The rapid attenuation of the mode when going away from the left surface is evident in the figure.

It was found that the inclusion of piezoelectricity did not modify the structure of the spectrum obtained in the purely elastic case, and only changes in the numerical values of the frequencies were produced, as a consequence of the different matching boundary conditions used when taking into account the piezoelectric coupling.

Thus it was found that the transverse elastic waves constitute a quite close parallel with the theoretical studies for one-dimensional 'simple' systems, and contrast with the case of the sagittal elastic waves [46], where the coupling of the different components of the elastic displacements makes the identification of the characteristics of the spectrum more difficult for the low-order generations studied in [46]. It was then clear that the study of the frequency spectrum of quasiregular systems for the sagittal elastic waves would be quite costly in computer time. This can easily be understood because when using Green function methods as in [46], the Green function of the system of N interfaces would be an $Nn \times Nn$ matrix, n being the size of the Green function matrices of the different materials forming the system, which depends on the model in question. If Nn is a large number, then heavy requirements are imposed on computer memory and time in inverting large matrices, which must be performed many times to obtain the frequency spectrum. This problem was overcome with the method introduced in [91,94] blending the transfer matrix and surface Green function matching methods. In this way one deals in practice with a two-interface problem instead an N-interface one, which reduces substantially the memory and computer time required. Instead of inverting many times the $Nn \times Nn$ matrices, one multiplies many times the N matrices of size $n \times n$ and then inverts a $2n \times 2n$ matrix.

By using this method, more general studies of the elastic waves in quasiregular systems were made [50,52,53]. In these studies the sagittal elastic waves for higher generation orders were studied, and other quasiregular sequences, like the Thue–Morse and the Rudin–Shapiro ones, were considered. These other sequences were not studied previously due to the fact that the number of terms in the sequence goes as 2^n, n being the order of the sequence, thus

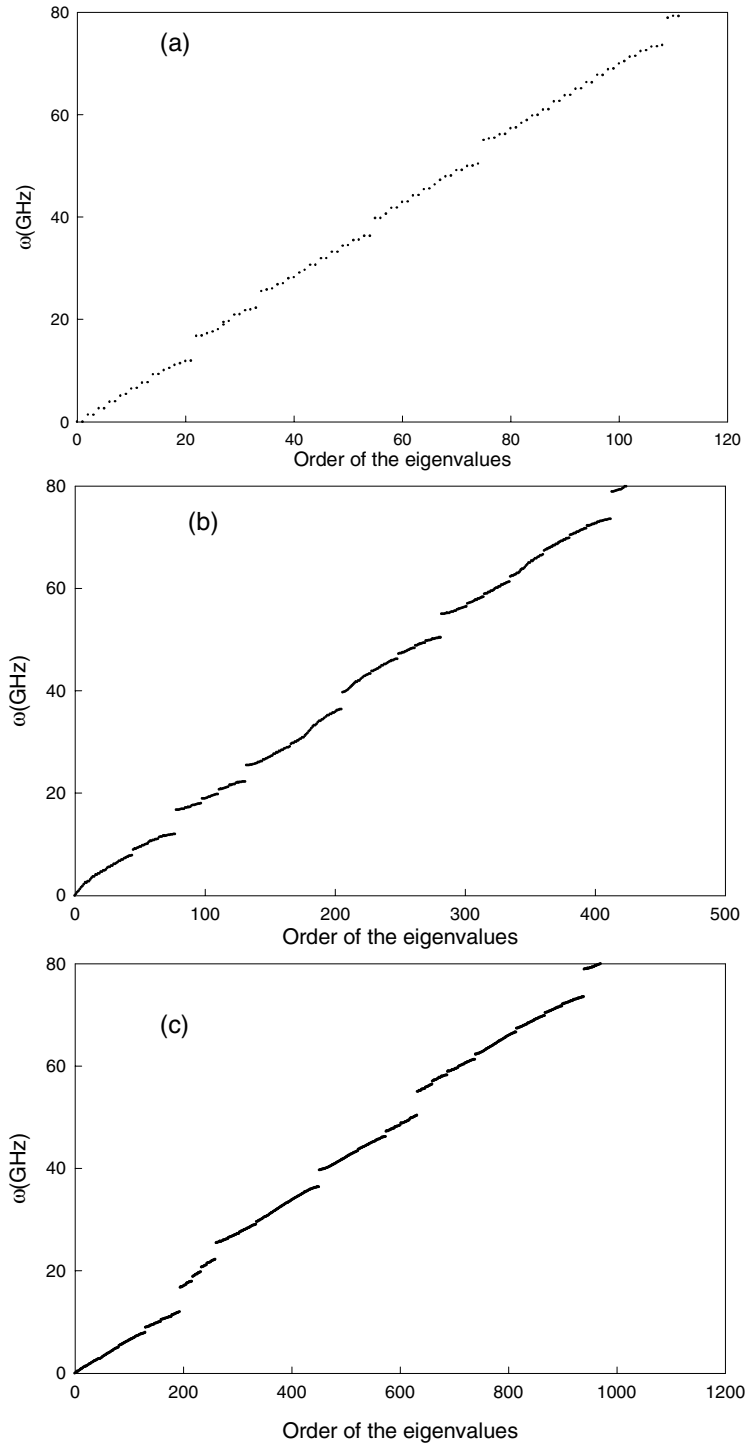

Figure 1. Transverse elastic wave frequencies ordered by increasing value versus the ordering number of the modes at the Γ point for periodic Fibonacci superlattices having as period: (*a*) the seventh generation; (*b*) the tenth generation; (*c*) the thirteenth generation. For the description of the constituent slabs, see the main text.

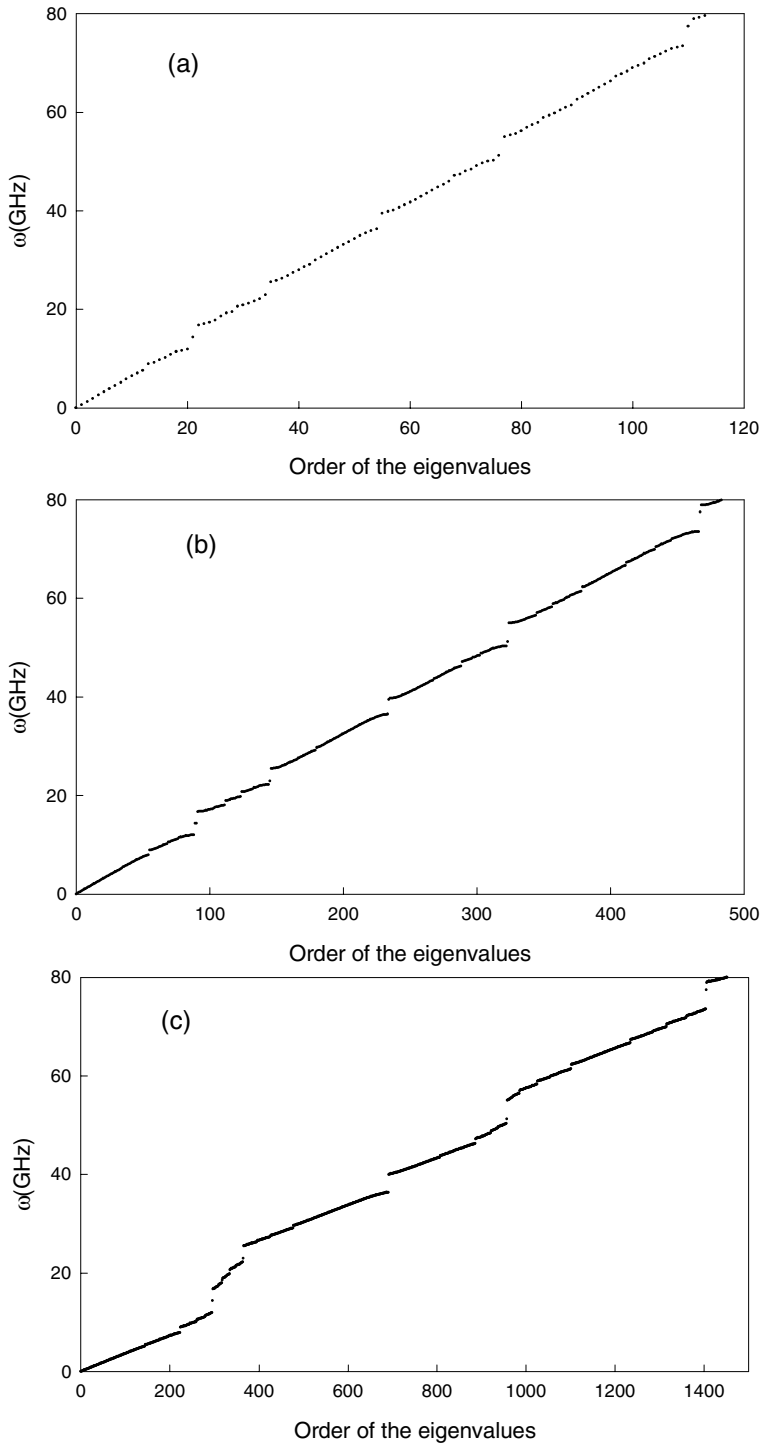

Figure 2. As figure 1, but for finite Fibonacci multilayers with stress-free surfaces.

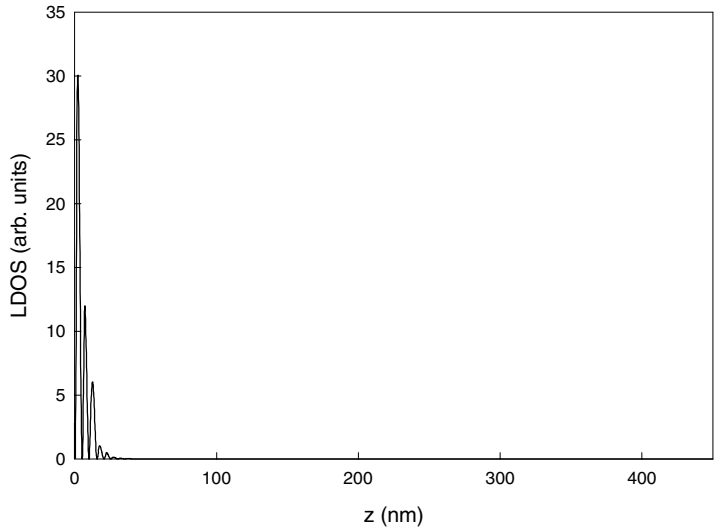

Figure 3. The LDOS in arbitrary units of the 14.37 GHz mode of the finite tenth-generation Fibonacci multilayer versus the length of the multilayer.

increasing the number of terms much more quickly than the Fibonacci sequence. The new technique allows now the study of systems with a high number of terms in a more economic way.

In [52] the Fibonacci and Thue–Morse systems were formed with two generators, blocks A and B, having $(\mathrm{AlAs})_i/(\mathrm{GaAs})_j$ layers and $(\mathrm{AlAs})_i/(\mathrm{GaAs})_k$ layers respectively. The thicknesses of the different layers were $d(\mathrm{AlAs}) = 17$ Å and $d(\mathrm{GaAs}) = 42$ Å for block A and $d(\mathrm{AlAs}) = 17$ Å and $d(\mathrm{GaAs}) = 20$ Å for block B.

The Rudin–Shapiro systems were formed with four generators, blocks A–D. The A- and B-blocks were the same as in the previous cases, while the C-block contained $(\mathrm{AlAs})_j/(\mathrm{GaAs})_i$ layers and the D-block contained $(\mathrm{AlAs})_k/(\mathrm{GaAs})_i$ layers. The thicknesses of the different layers were $d(\mathrm{AlAs}) = 42$ Å and $d(\mathrm{GaAs}) = 17$ Å for block C and $d(\mathrm{AlAs}) = 20$ Å and $d(\mathrm{GaAs}) = 17$ Å for block D.

The study included Fibonacci generations ranging from the second to the 14th, including up to 1220 slabs of constituent materials in the case of the 14th generation. The Thue–Morse and Rudin–Shapiro structures ranged from the first to the ninth, including up to 1024 slabs of constituent materials in the case of the ninth generation.

All the systems considered in [52] were finite structures with stress-free bounding surfaces.

Figure 4 presents a range of frequencies versus its ordering number for increasing frequencies of transverse elastic waves at the $\bar{\Gamma}$ point of:

(a) the 14th Fibonacci generation;
(b) the 9th Thue–Morse generation; and
(c) the 9th Rudin–Shapiro generation.

It is evident in the figure that all the structures exhibit spectrum fragmentation, manifested by the presence of primary and secondary gaps. The isolated points in the gaps are localized states, due to the existence of stress-free bounding surfaces. The figure evidences the similarities of the Fibonacci and Thue–Morse spectra, while the Rudin–Shapiro structure presents a spectrum showing clear differences.

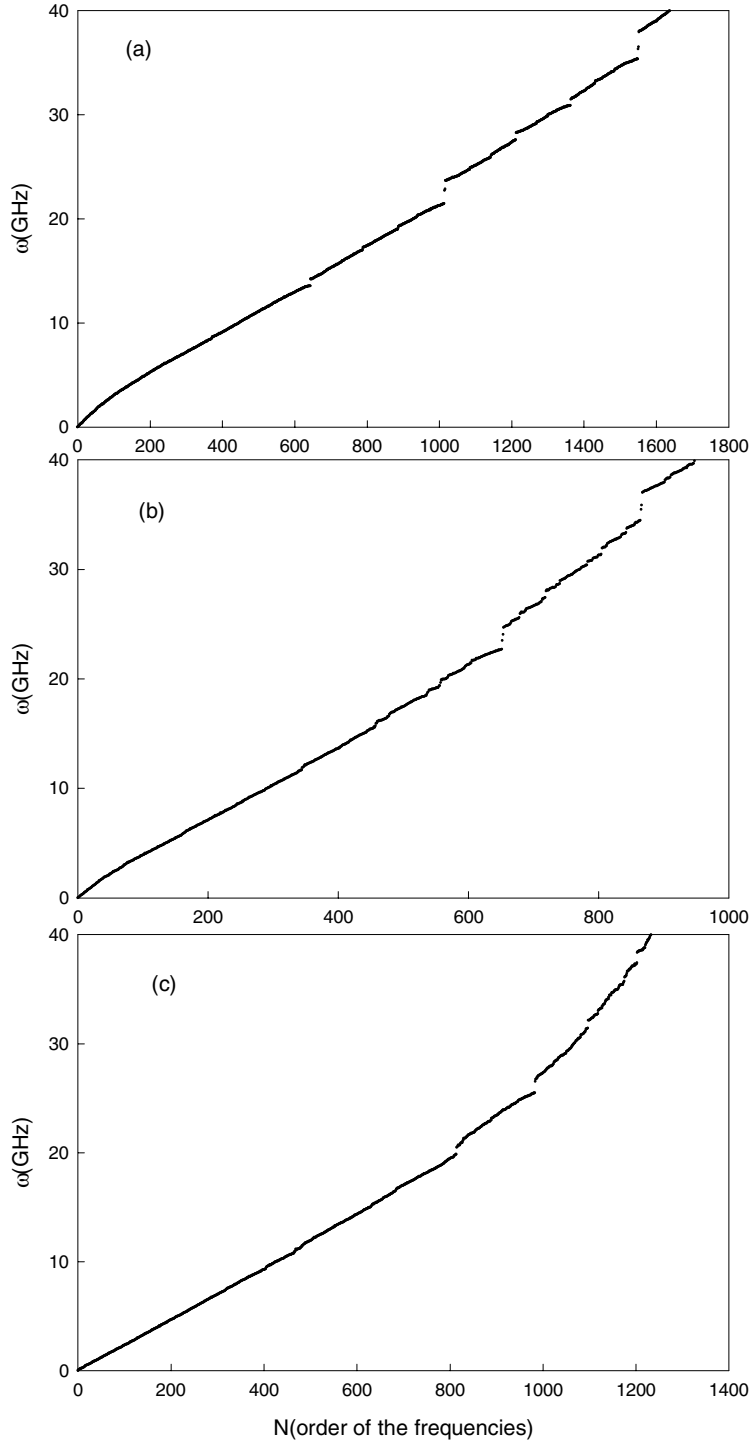

Figure 4. Transverse elastic wave frequencies ordered by increasing value versus ordering number of modes for the $\bar{\Gamma}$ point of finite multilayers with stress-free surfaces: (*a*) 14th Fibonacci generation; (*b*) 9th Thue–Morse generation; and (*c*) 9th Rudin–Shapiro generation.

Figure 5 presents the same information as figure 4 for the sagittal elastic waves of the 14th Fibonacci generation. The spectrum fragmentation is not easily seen in figure 5(*a*), as found in [46], despite having higher generations than those in [46]. But at the $\bar{\Gamma}$ point the longitudinal and transverse contributions to the sagittal waves can be decoupled and this allows one to see the spectrum fragmentation. Figure 5(*b*) gives this information for the longitudinal part of the sagittal elastic wave, while figure 5(*c*) displays the information for the transverse part of the sagittal elastic wave. Figures 5(*b*) and (*c*) exhibit the spectrum fragmentation in a clear way, which is not the case for lower generations, as found in [46]. A similar situation was found in [52] for the sagittal elastic waves in Thue–Morse and Rudin–Shapiro heterostructures. In any case the conclusions presented in [46] for low-order generations are valid, and spectrum fragmentation will not appear in situations where wave mixing is quite strong, like that occurring for arbitrary propagation directions in anisotropic crystals.

In spite of the apparent self-similar structures seen in the previous figures, it can be seen that this is not true. This is evident in figure 6 giving the same information as was presented in figure 4 for the 14th Fibonacci generation, but for different ranges of frequencies. These magnifications show the existence of primary and secondary gaps as before, but no self-replicating structure is present in any of the sequences. This can also be seen in Thue–Morse and Rudin–Shapiro heterostructures [52].

The character of the different modes is reflected through the LDOS versus the length of the multilayer. Figure 7 depicts the LDOS in arbitrary units of the transverse elastic waves with frequencies (*a*) 34.5, (*b*) 36.1, and (*c*) 37.0 GHz, for the sixth Thue–Morse generation, including 128 constituent materials, versus the length of the multilayer system. The extended character of the (*a*) and (*c*) modes is evident, while the localized character of the (*b*) mode is clear from the rapid attenuation of the mode, when receding from the right surface. Similar trends were found for the Fibonacci structures [52].

Figure 8 shows the LDOS of the transverse elastic waves with frequencies: (*a*) 36.9, (*b*) 37.8, and (*c*) 38.2 GHz, of the sixth Rudin–Shapiro generation, including 128 constituent materials, versus the length of the multilayer system. The marked differences in behaviour between the various modes and the equivalent modes obtained for the Fibonacci and Thue–Morse sequences are evident in this case.

Other studies on the influence of the boundary conditions and the constituent building blocks were made in [50, 53]. In [53] two types of building block were considered. The first one, denoted as case I, had the same building blocks as those considered in [52]. The second case, denoted as II, considered *A*-blocks formed by GaAs layers and *B*-blocks formed by AlAs layers with thicknesses $d(\mathrm{AlAs}) = 17$ Å and $d(\mathrm{GaAs}) = 42$ Å, respectively, for the Fibonacci, Thue–Morse, and Rudin–Shapiro systems considered there. The Rudin–Shapiro II structures had *C*-blocks formed by GaAs layers and *D*-blocks formed by AlAs layers, with thicknesses $d(\mathrm{AlAs}) = 20$ Å and $d(\mathrm{GaAs}) = 17$Å.

Different quasiregular generations were studied including up to 2048 constituent material slabs. Different mathematical tools were employed to study the frequency spectrum. Because the different systems had different numbers of constituent slab materials, the frequency spectra were presented by means of the normalized integrated density of states (NIDOS), normalized to unity. This gives a completely equivalent representation and provides a better picture of the results of the different structures containing different numbers of material slabs, and thus of frequency eigenvalues.

Figure 9 gives the NIDOS as a function of the frequency for two realizations of a 13th Fibonacci generation corresponding to case I. The solid curve corresponds to the Γ point of a periodic superlattice having the Fibonacci sequence as the period. The dashed curve corresponds to the $\boldsymbol{\kappa} = (10^5, 0)$ m^{-1} point of the finite sequence with stress-free bounding

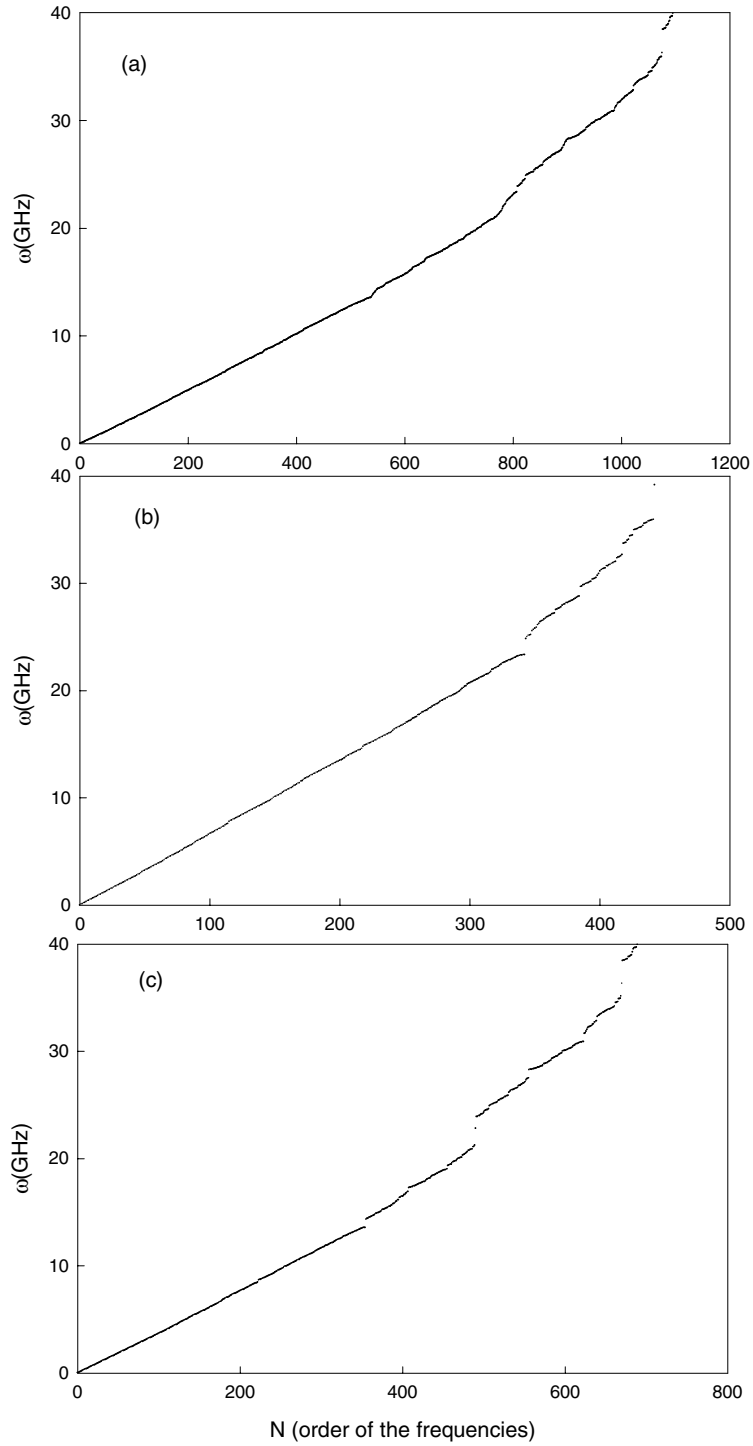

Figure 5. Elastic wave frequencies ordered by increasing value versus ordering number of modes for the $\bar{\Gamma}$ point of a finite 14th Fibonacci generation with stress-free surfaces: (*a*) sagittal elastic waves; (*b*) the longitudinal contribution to sagittal elastic waves; (*c*) the transverse contribution to sagittal elastic waves.

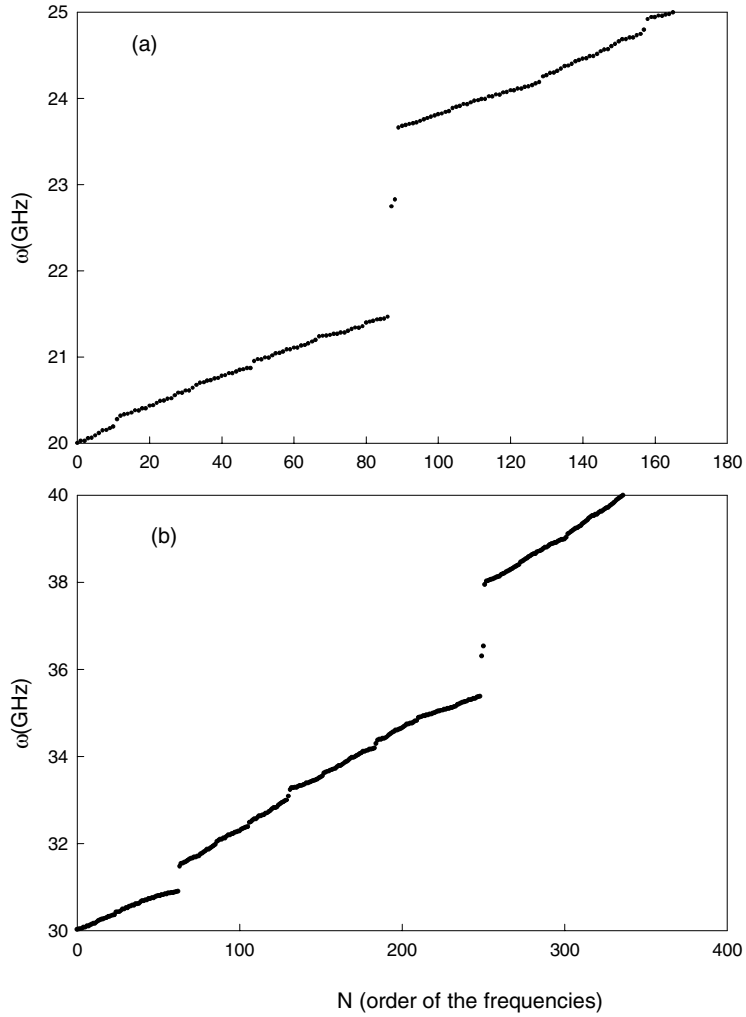

Figure 6. Transverse elastic wave frequencies ordered by increasing values versus ordering number of modes for the $\bar{\Gamma}$ point of a finite 14th Fibonacci generation with stress-free surfaces: (*a*) the frequency range 20 GHz $\leqslant \omega \leqslant$ 25 GHz; (*b*) the frequency range 30 GHz $\leqslant \omega \leqslant$ 40 GHz.

surfaces. It is easy to see that in spite of having chosen not only different boundary conditions, but even different $\boldsymbol{\kappa}$-points in the two cases, the spectra in both situations are almost identical, and they exhibit the same features. The largest differences correspond to the low-frequency limit, as can easily be understood. At the Γ point the frequency starts from zero, whereas for the non-zero $\boldsymbol{\kappa}$-point the frequency starts at a non-zero value.

Figure 10 presents the same information for two different realizations of the 13th Fibonacci generation in case II, for the $\boldsymbol{\kappa} = (10^5, 0)$ m^{-1} point of the finite sequence with stress-free bounding surfaces. The dashed curve represents the case in which the A-block corresponds to GaAs and the B-block corresponds to AlAs, whereas the solid line corresponds to the reverse situation. It can be seen that the overall features are the same, although some small differences are evident in the figure. Not so many gaps are present as in the previous figure. This is a consequence of the smaller number of material slabs included in the generation.

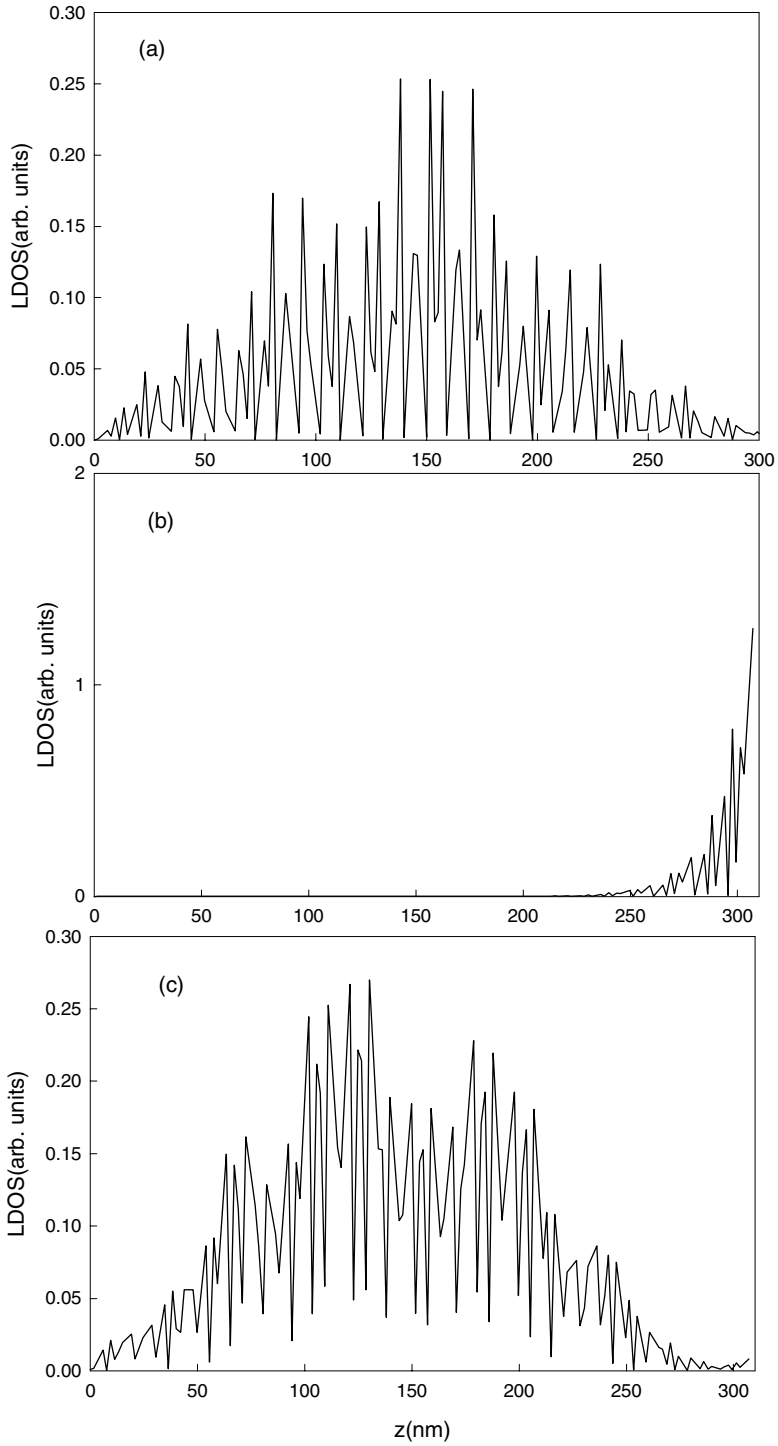

Figure 7. The spatial dependence of the LDOS in arbitrary units, for frequencies of: (*a*) 34.5 GHz; (*b*) 36.1 GHz; and (*c*) 37.0 GHz, for transverse elastic modes of the finite sixth Thue–Morse generation.

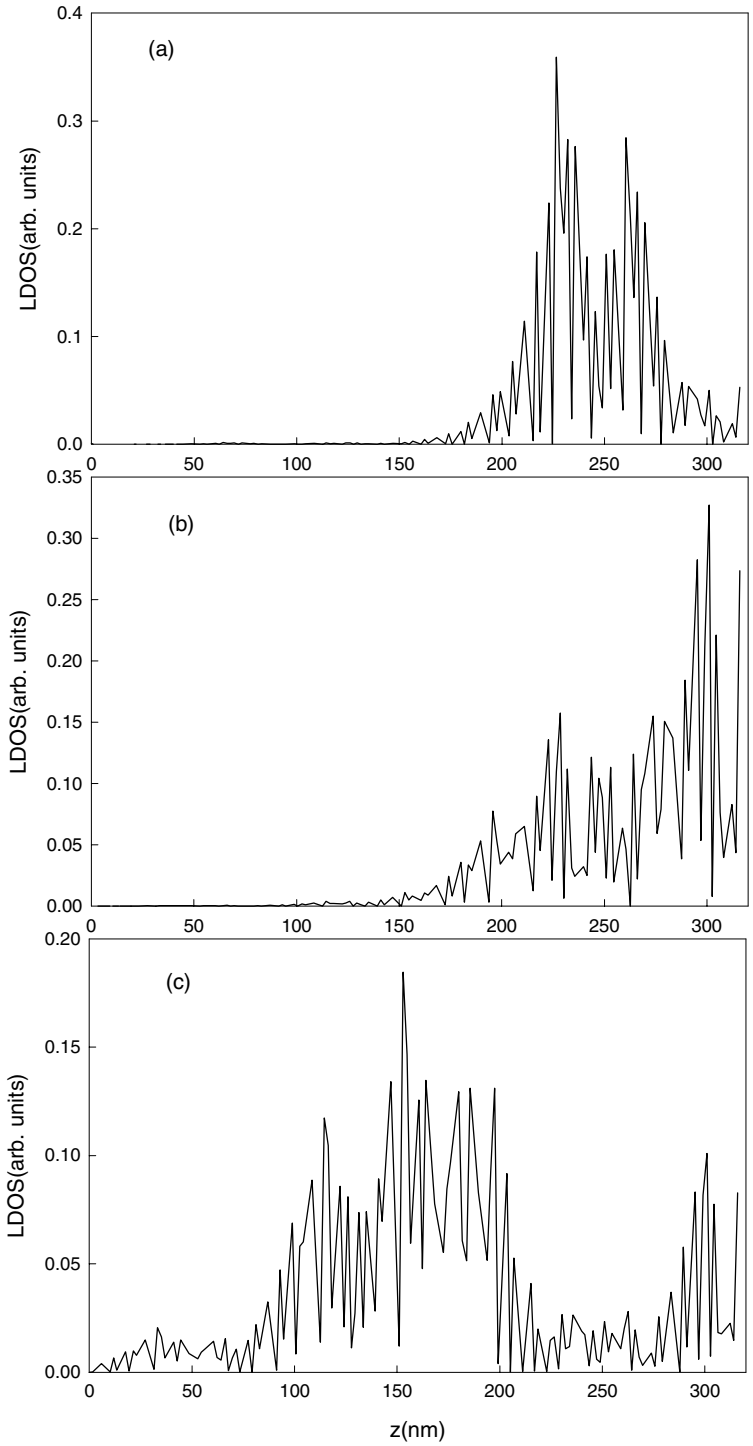

Figure 8. As figure 7, but for: (*a*) 36.9 GHz; (*b*) 37.8 GHz; and (*c*) 38.2 GHz, transverse elastic modes of the finite sixth Rudin–Shapiro multilayer.

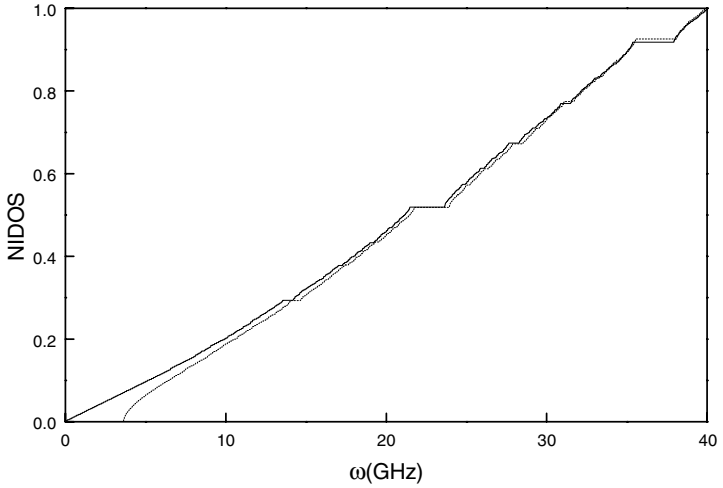

Figure 9. The NIDOS as a function of the frequency for the 13th Fibonacci generation, case I. Solid curve: the Γ point of the infinite periodic system. Dashed curve: the finite system with stress-free bounding surfaces and $\boldsymbol{\kappa} = (10^5, 0)\ \mathrm{m}^{-1}$.

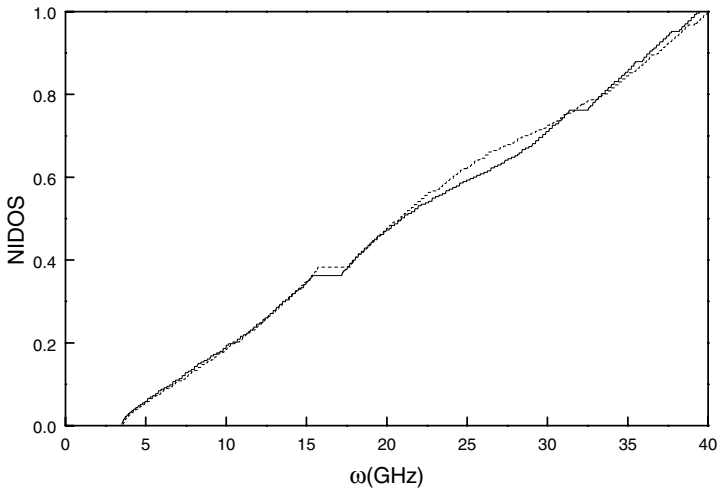

Figure 10. As figure 9, but for case II of the 13th-Fibonacci-generation finite systems with stress-free bounding surfaces and $\kappa = (10^5, 0)\ \mathrm{m}^{-1}$. Dashed curve ($A \longleftrightarrow$ GaAs, $B \longleftrightarrow$ AlAs); solid curve ($A \longleftrightarrow$ AlAs, $B \longleftrightarrow$ GaAs).

As a complement to the study of the frequency spectra a fractal analysis of them was also performed in [53] by means of the generalized box-counting dimension $D(q)$ discussed in section 3.

Figure 11 gives $D(q)$ for the systems considered in figures 12, 13. It is seen that the behaviour is the same for all systems, and that the $+\infty$ limits are very close for the I systems and the two II systems, although there is a clear difference between the limiting values for the I and II types. It was also seen in [53] that the Thue–Morse systems, although exhibiting differences with respect to the Fibonacci ones, had quite similar trends, as previously seen in [52].

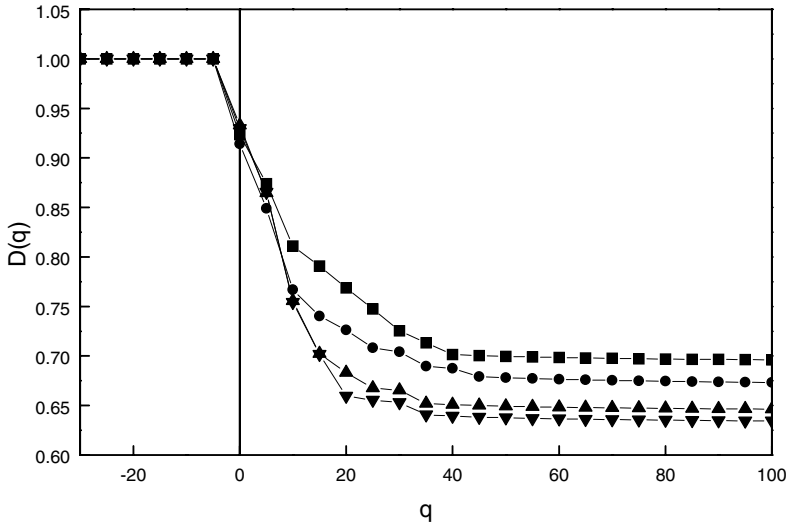

Figure 11. The generalized box-counting fractal dimension $D(q)$ for the 13th Fibonacci generation (●: infinite periodic case I; ■: finite case I; ▲: finite case II ($A \longleftrightarrow$ GaAs, $B \longleftrightarrow$ AlAs); ▼: finite case II ($A \longleftrightarrow$ AlAs, $B \longleftrightarrow$ GaAs)).

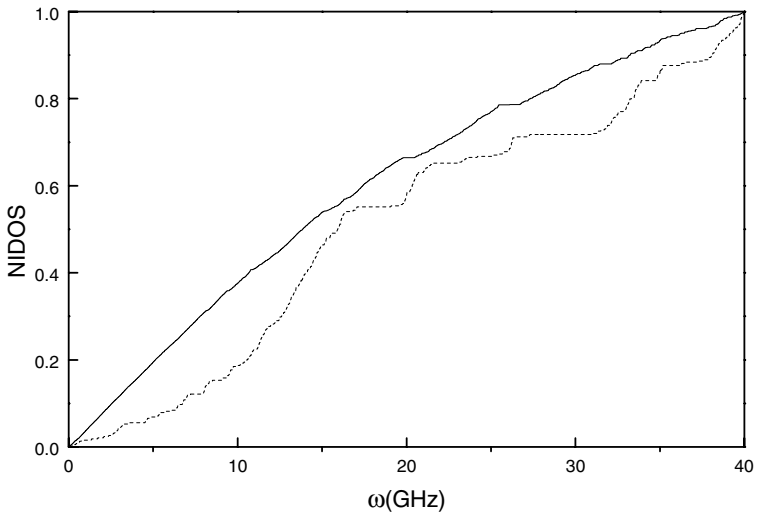

Figure 12. As figure 9, but for the tenth-Rudin–Shapiro-generation finite system with stress-free bounding surfaces. Solid curve: case I. Dashed curve: case II ($A, C \longleftrightarrow$ GaAs; $B, D \longleftrightarrow$ AlAs).

Figure 12 gives the NIDOS as a function of the frequency for two realizations of the tenth Rudin–Shapiro generation with stress-free bounding surfaces. The solid curve corresponds to case I with 2048 constituent material slabs, and the dashed line corresponds to case II having 1024 constituent material slabs. In this case the two different types exhibit quite different features, more pronounced than those seen in the Fibonacci and Thue–Morse structures.

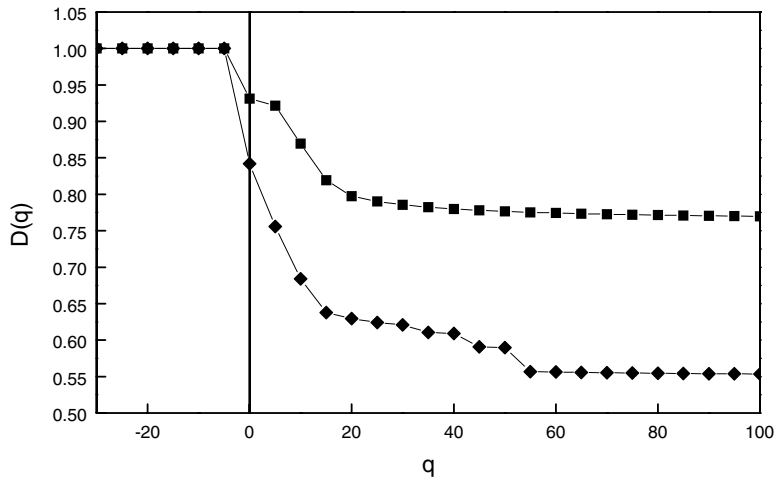

Figure 13. As figure 11, but for the tenth-Rudin–Shapiro-generation finite structure with stress-free bounding surfaces (■: case I; ♦: case II (A, C ⟷ GaAs; B, D ⟷ AlAs)).

Figure 13 gives $D(q)$ for the systems considered in the previous figure. The behaviour of the I system is similar to that seen for the I systems in the Fibonacci and Thue–Morse structures, although the $+\infty$ limit is higher in the Rudin–Shapiro case. The behaviour of the II system is similar to that of the Thue–Morse case, although the $+\infty$ limit is reached earlier in the Rudin–Shapiro case. The difference between the $+\infty$ limits of the I and II cases is larger than for the Fibonacci and Thue–Morse structures.

The conclusions reached when studying elastic waves in quasiregular systems are similar to those obtained for polar optical modes in Fibonacci heterostructures [48]. The model employed in [48] was a realistic one, taking full account of all couplings at any value of κ [105, 106], including the electrostatic potential and vibrational amplitudes.

5. Conclusions; open questions

Quasiregular systems are attractive and intriguing, and a great deal of literature has been generated.

The mathematical analysis can be very useful for providing formal guidance, but until now has been restricted to simple problems with 2×2 transfer matrices. To our knowledge there is no trace map available for a higher-rank transfer matrix, which is necessary to cover many physical models involving more than one amplitude. Further work on this subject is needed.

Many studies with 'simple' models have been made which appear to exhibit some self-similarity. However, trifurcation is simply a qualitative feature, and a property needs precise adequate concepts for its definition and well defined parameters for its quantitative description. All that is known from general theory is

(i) that a self-similar object must be fractal and
(ii) that in *multifractal* spectra there are different inherent scales, but this has not been so far translated into useful concepts for analysing the situation in morphological terms.

All this leaves the field open for numerical experiments in 'simple' and 'real' systems, in order to clarify some relevant issues.

The study of elastic waves in quasiregular systems can be seen as an economical approach to the study of 'real' quasiregular systems. It provides us with a kind of parallel of the one-dimensional 'simple' systems (the transverse elastic waves) and with a more complicated situation without analogue in the 'simple' systems (the sagittal elastic waves).

In this way it has been found that the frequency spectra exhibit the usual pattern of primary and secondary gaps and they have multifractal character. It has also been seen that there is no symptom of anything resembling a self-similar pattern of trifurcations for the different generations of quasiregular systems studied [46–48, 50, 52–54].

These results are all in line with the remark stressed in [29] that fractal character and self-similarity are properties of a fundamentally different nature which need not always be associated, except for eigenvalue problems with the simplest mathematical structure. The fractal character is a more basic topological property: it appears quite generally as a consequence of the quasiregular geometrical structure and it admits a precisely defined quantitative measure. The self-similarity is an essentially different property of a morphological nature for which precise quantitative definitions appear to be generally lacking, except for the simplest ideal cases, and even taken as a qualitative concept it is usually loosely defined and often remains largely a matter of visual appreciation.

The influence of the boundary conditions (periodic or stress-free types) does not seem to be very important beyond the appearance of localized modes in the primary and secondary gaps in the case of the stress-free boundary conditions. In all the cases studied it has been seen that $D(q)$ varies with q, thus indicating that the spectrum is not only fractal, but *multifractal* and therefore there are different scaling factors. This rules out strict self-similarity, although some partial results, partially considered, might have a self-similar appearance.

The study of the sagittal elastic waves has shown that the spectrum fragmentation will not appear in situations where wave mixing is quite strong, such as that occurring for arbitrary propagation directions in anisotropic crystals [46].

It has also been seen that the frequency spectra of Fibonacci and Thue–Morse systems have many similarities. On the other hand the Rudin–Shapiro systems, not covered by the mathematical theorems [59,65] for 'simple' models, present important differences with respect to the former systems and leave many questions unanswered.

It must be stressed that while many theoretical studies have been performed, not much experimental information is available on quasiregular systems.

Possible applications of quasiregular systems as frequency-doubling devices have been noted [56, 107–111]. It is clear that more work on the properties of 'real' quasiregular systems is still needed.

Acknowledgments

One of the authors (RPA) gratefully acknowledges the hospitality of the Jaume I University where part of this work was done. This work was partially supported by the Spanish Ministry of Science and Technology through grant BFM2000-1330 and the Spanish–Cuban agreement CSIC-CITMA.

References

[1] Shechtman D, Blech I, Gratias D and Cahn J W 1984 *Phys. Rev. Lett.* **53** 1951
[2] Shechtman D and Blech I 1985 *Metall. Trans.* A **16** 1005
[3] He L X, Li X Z, Zhang Z and Kuo K H 1988 *Phys. Rev. Lett.* **61** 1116
[4] Goldman A I and Ketton R F 1993 *Rev. Mod. Phys.* **65** 213
[5] Esaki L 1984 *J. Physique Coll.* **45** C5 3
[6] Vinter B and Weisbuch C 1991 *Quantum Semiconductor Structures* (San Diego, CA: Academic)
[7] Gossard A C, Miller R C and Weigman W 1986 *Surf. Sci.* **174** 131
[8] Merlin R, Bajema K, Clarke R, Juang F-Y and Bhattacharya P K 1985 *Phys. Rev. Lett.* **55** 1768

[9] Todd J, Merlin R, Clarke R, Mohanty K M and Axe J D 1986 *Phys. Rev. Lett.* **57** 1157
[10] Merlin R, Bajema K, Nagle J and Ploog K 1987 *J. Physique Coll.* **48** C5 503
[11] Hurley D C, Tamura S and Wolfe J P 1988 *Phys. Rev.* B **37** 8829
[12] Kohmoto M, Kadanoff L P and Tang C 1983 *Phys. Rev. Lett.* **50** 1870
[13] Kohmoto M and Ono Y 1984 *Phys. Lett.* A **102** 145
[14] Halsey T C, Jansen M H, Kadanoff L P, Procaccia I and Shraiman R I 1986 *Phys. Rev.* A **33** 1141
[15] Lu J P, Odagaki T and Birman J L 1986 *Phys. Rev.* B **33** 4809
[16] Kohmoto M and Banavar J R 1986 *Phys. Rev.* B **34** 563
[17] Nori F and Rodriguez J P 1986 *Phys. Rev.* B **34** 2207
[18] Kohmoto M 1986 *Phys. Rev.* B **34** 5043
[19] Niu Q and Nori F 1986 *Phys. Rev. Lett.* **57** 2057
[20] Fujita M and Machida K 1986 *Solid State Commun.* **59** 61
[21] Kohmoto M, Sutherland B and Tang C 1987 *Phys. Rev.* B **35** 1020
[22] Luck J M 1989 *Phys. Rev.* B **39** 5834
[23] Kaplan D E and Glass L 1995 *Understanding Nonlinear Dynamics* (New York: Springer)
[24] Ostlund S, Pandit R, Rand D, Schellnhuber H J and Siggia E D 1983 *Phys. Rev. Lett.* **50** 1873
[25] Minomiya T 1996 *J. Phys. Soc. Japan* **55** 3709
[26] Liu Y and Riklund R 1987 *Phys. Rev.* B **35** 6034
[27] Tamura S and Wolfe J P 1987 *Phys. Rev.* B **36** 3491
[28] Maciá E and Domínguez-Adame F 2000 *Electrons, Phonons and Excitons in Low Dimensional Aperiodic Systems* (Madrid: Editorial Complutense)
[29] Pérez-Alvarez R and García-Moliner F 2001 The spectrum of quasiregular heterostructures *Some Contemporary Problems of Condensed Matter Physics* ed S J Vlaev and L M Gaggero-Sager (New York: Nova Science) p 1
[30] Tamura S and Nori F 1990 *Phys. Rev.* B **41** 7941
[31] Niu Q and Nori F 1990 *Phys. Rev.* B **42** 10 329
[32] Huang D, Gumbs G and Kolář M 1992 *Phys. Rev.* B **46** 11 479
[33] Munzar D, Bročáev L, Humlíček J and Ploog K 1994 *J. Phys.: Condens. Matter* **6** 4107
[34] Maciá E, Domínguez-Adame F and Sánchez A 1994 *Phys. Rev.* E **50** R679
[35] Carpena P, Gasparian V and Ortuño M 1995 *Phys. Rev.* B **51** 12 813
[36] Domínguez-Adame F, Maciá E, Méndez B, Roy C L and Khan A 1995 *Semicond. Sci. Technol.* **10** 797
[37] Huang D, Gumbs G, Zhao Y and Auner G W 1995 *Phys. Lett.* A **200** 459
[38] Hirose K, Ho D Y K and Kamimura H J 1992 *J. Phys.: Condens. Matter* **4** 5947
[39] Jing G J, Kang S S, Wang Z D, Hu A and Jiang S S 1996 *Phys. Rev.* B **54** 11 883
[40] You J Q, Zhang L and Yang Q B 1997 *Phys. Rev.* B **55** 1314
[41] Arriaga J and Velasco V R 1997 *Physica* A **241** 377
[42] Arriaga J and Velasco V R 1997 *J. Phys.: Condens. Matter* **9** 8031
[43] Oh G Y 1998 *J. Korean Phys. Soc.* **33** 617
[44] Tong P Q 1998 *Physica* B **254** 212
[45] Sibilia C, Tropea F and Bertolotti M J 1998 *J. Mod. Opt.* **45** 2255
[46] Fernández-Alvarez L and Velasco V R 1998 *Phys. Rev.* B **57** 14 141
[47] Zárate J E, Fernández-Alvarez L and Velasco V R 1999 *Superlatt. Microstruct.* **25** 519
[48] Pérez-Alvarez R, García-Moliner F, Trallero-Giner C and Velasco V R 2000 *J. Raman Spectrosc.* **31** 421
[49] Velhinho M T and Pimentel I R 2000 *Phys. Rev.* B **61** 1043
[50] Pérez-Alvarez R, García-Moliner F and Velasco V R 2001 *J. Phys.: Condens. Matter* **13** 3689
[51] Maciá E 2001 *Phys. Rev.* B **63** 205421
[52] Velasco V R and Zárate J E 2001 *Prog. Surf. Sci.* **67** 383
[53] Tutor J and Velasco V R 2001 *Int. J. Mod. Phys.* B **21** 2925
[54] Velasco V R 2002 *Microelectron. J.* **33** 361
[55] Peyriere J, Cockayne E and Axel F 1995 *J. Physique* **5** 111
[56] Zhu S-U, Zhu Y-Y and Ming N-B 1997 *Science* **278** 843
[57] Liu X, Wang Z, Wu J, Shen D and Ming N 1998 *Phys. Rev.* B **58** 12 782
[58] Bellissard J, Iochum B, Scoppola E and Testard D 1989 *Commun. Math. Phys.* **125** 527
[59] Sütő A 1989 *J. Stat. Phys.* **56** 525
[60] Bellissard J, Bovier A and Ghez J M 1991 *Commun. Math. Phys.* **135** 379
[61] Bellissard J, Iochum B and Testard D 1993 *Commun. Math. Phys.* **141** 353
[62] Bellissard J, Bovier A and Ghez J M 1992 *Rev. Math. Phys.* **4** 1
[63] Bovier A 1992 *J. Phys. A: Math. Gen.* **25** 1021
[64] Bovier A and Ghez J M 1993 *Commun. Math. Phys.* **158** 45

[65] Bovier A and Ghez J M 1995 *J. Phys. A: Math. Gen.* **28** 2313
[66] Kolář M and Nori F 1990 *Phys. Rev.* B **42** 1062
[67] Thue A 1906 *Norske Vidensk. Selsk. Skr.* I **7** 1
Morse M 1921 *Trans. Am. Math. Soc.* **22** 84
[68] Rudin W 1959 *Proc. Am. Math. Soc.* **10** 855
Shapiro H S 1951 *Master's Thesis* MIT, Cambridge, MA
[69] Hof A, Krill O and Simon B 1995 *Commun. Math. Phys.* **174** 149
[70] James H M 1949 *Phys. Rev.* **76** 1602
[71] Strandberg M W P 1982 *Phys. Rev.* B **25** 5147
[72] Smith R A 1961 *Wave Mechanics of Crystalline Solids* (New York: Wiley)
[73] Mora M E, Pérez R and Sommers Ch B 1985 *J. Physique* **46** 1021
[74] Baxter R J 1982 *Exactly Solved Models in Statistical Mechanics* (London: Academic)
[75] Lieb E H and Mattis D C 1966 *Mathematical Physics in One Dimension: Exactly Soluble Models of Interacting Particles* (New York: Academic)
[76] Mattis D C 1993 *The Many-Body Problem: an Encyclopedia of Exactly Solved Models in One Dimension* (Singapore: World Scientific)
[77] Baake M, Grimm U and Joseph D 1993 *Int. J. Mod. Phys.* B **7** 1527
[78] Bellissard J, Bovier A and Ghez J M 1993 *Math. Sci. Eng.* **192** 13
[79] Hof A 1993 *J. Stat. Phys.* **72** 1353
[80] Roberts J A G and Baake M 1994 *NATO ASI Ser. B Hamiltonian Mechanics: Integrability and Chaotic Behaviour vol 331* (New York: Plenum) p 275
[81] Jitomirskaya S Ya and Last Y 1996 *Phys. Rev. Lett.* **76** 1765
[82] Rudinger A and Sire C 1996 *J. Phys. A: Math. Gen.* **29** 3537
[83] Damanik D 1997 *Univ. Iagel. Acta Math.* **34** 45
[84] Hof A 1997 *Commun. Math. Phys.* **184** 567
[85] Damanik D 1998 *Helv. Phys. Acta* **71** 667
[86] Damanik D 1998 *Lett. Math. Phys.* **46** 303
[87] Damanik D 1998 *Commun. Math. Phys.* **196** 477
[88] Gazean J P and Miekisz J 1998 *J. Phys. A: Math. Gen.* **31** L435
[89] Poisson O 1999 *Math. Methods Appl. Sci.* **22** 773
[90] Barnett S 1990 *Matrices. Methods and Applications* (Oxford: Oxford University Press)
[91] García-Moliner F and Velasco V R 1992 *Theory of Single and Multiple Interfaces. The Surface Green Function Matching Method* (Singapore: World Scientific)
[92] Pérez-Alvarez R, García-Moliner F and Velasco V R 1995 *J. Phys.: Condens. Matter* **7** 2037
[93] Fernández-Alvarez L, Monsivais G, Vlaev S and Velasco V R 1996 *Surf. Sci.* **369** 367
[94] Velasco V R 2001 Study of many interfaces and inhomogeneous systems by means of surface Green function matching and transfer matrix methods *Contemporary Problems of Condensed Matter Physics* ed S Vlaev and L M Gaggero-Sager (New York: Nova Science) p 133
[95] Moon F C 1992 *Chaotic and Fractal Dynamics* (New York: Wiley-Interscience)
[96] Ott E O 1993 *Chaos in Dynamical Systems* (Cambridge: Cambridge University Press)
[97] Hilborn R C 1994 *Chaos and Nonlinear Dynamics* (Oxford: Oxford University Press)
[98] Rasband S N 1997 *Chaos Dynamics of Nonlinear Systems* (New York: Wiley)
[99] Bajema K and Merlin R 1987 *Phys. Rev.* B **36** 4555
[100] Lockwood D J, Macdonald A H, Aers G C, Dharma-Wardana M W C, Devine R L S and Moore W T 1987 *Phys. Rev.* B **36** 9286
[101] Dharma-Wardana M W C, Macdonald A H, Lockwood D J, Baribeau J M and Houghton D C 1987 *Phys. Rev. Lett.* **58** 1761
[102] Bleustein J L 1968 *Appl. Phys. Lett.* **13** 412
[103] Gulyaev Yu V 1969 *JETP Lett.* **9** 63
[104] Dieulesaint E and Royer D 1980 *Elastic Waves in Solids* (Chichester: Wiley)
[105] Pérez-Alvarez R, García-Moliner F, Velasco V R and Trallero-Giner C 1993 *J. Phys.: Condens. Matter* **5** 5389
[106] Trallero-Giner C, Pérez-Alvarez R and García-Moliner F 1998 *Long Wave Polar Modes in Semiconductor Heterostructures* (Oxford: Pergamon)
[107] Zhu Y-Y and Ming N-B 1990 *Phys. Rev.* B **42** 3676
[108] Zhu S-N, Zhu Y-Y, Qin Y-Q, Ge C-Z and Ming N-b 1997 *Phys. Rev. Lett.* **78** 2752
[109] Liu X, Wang Z, Wu J, Shen D and Ming N 1998 *Phys. Rev.* B **58** 12 782
[110] Chen Y-B, Zhu Y-Y, Qin Y-Q, Zhang C, Zhu S-N and Ming N-B 2000 *J. Phys.: Condens. Matter* **12** 529
[111] Yang X and Liu Y 2000 *J. Phys.: Condens. Matter* **12** 1899